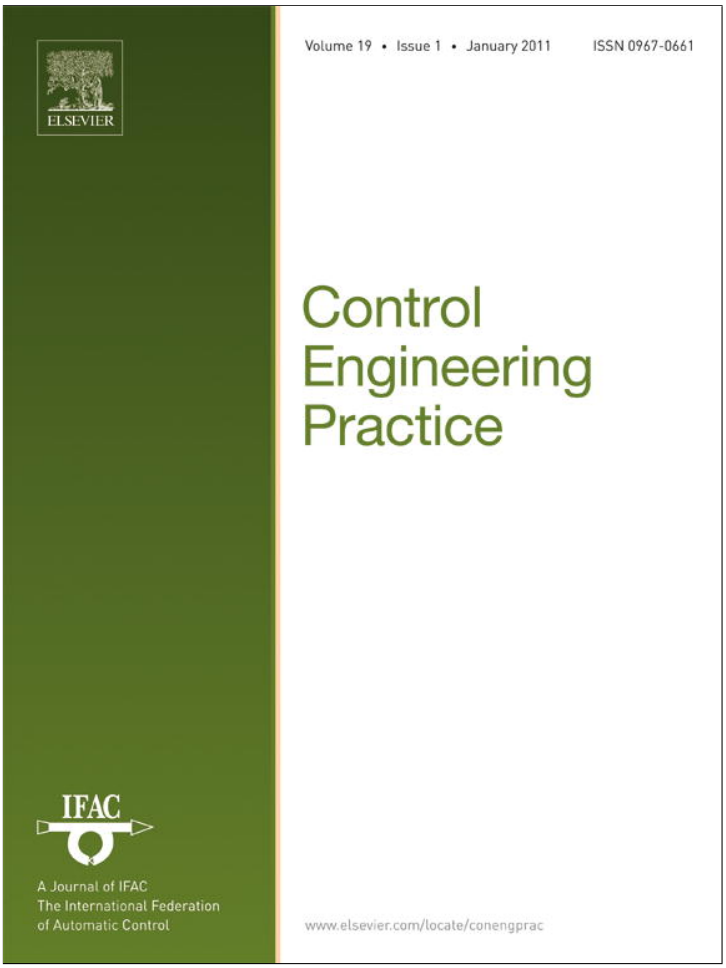

Control Engineering Practice 19 (2011) 1–9

Contents lists available at ScienceDirect

Control Engineering Practice

journal homepage: www.elsevier.com/locate/conengprac

Model predictive control of a rotary cement kiln

Konrad S. Stadler [a,*], Jan Poland [a], Eduardo Gallestey [b]

[a] ABB Switzerland Ltd, Corporate Research, Baden-Dättwil, Switzerland
[b] ABB Switzerland Ltd, Process Automation Division, Baden-Dättwil, Switzerland

ARTICLE INFO

Article history:
Received 29 March 2010
Accepted 24 August 2010
Available online 19 September 2010

Keywords:
Rotary cement kiln
Model predictive control
Moving horizon estimation
First principles model
Compartmental model

ABSTRACT

A first principles model of a cement kiln is used to control and optimize the burning of clinker in the cement production process. The model considers heat transfer between a gas and a feed state via convection and radiation. Furthermore, it contains effects such as chemical reactions, feed transport, energy losses and energy input. A model predictive controller is used to stabilize a temperature profile along the rotary kiln, guarantee good combustion conditions and maximize production. Moving horizon estimation was used for online estimation of selected model parameters and unmeasured states. Results from the pilot site are presented.

1. Introduction

In a cement plant the clinker production is of major importance as the quality of the cement greatly depends on the quality of the clinker. The clinker production process can be roughly split into four sequential subprocesses: preheating, calcining, sintering (or burning, formation of clinker minerals) and cooling. However, many different plant configurations with different types of rotary kilns, preheater cyclone configurations, with or without precalciner, with or without tertiary air duct, etc. are known. Typically, the configuration depends strongly on the available raw material, the available fuels and the plant evolution driven by the progress of the cement production technologies. A number of examples of possible configurations can be found in Peray (1986).

The approach described in this work provides a generic method to model and control any type of cement clinker production line. This is important as the engineering and commissioning of controllers in an industrial setting are costly. Therefore, it is proposed to divide the models into generic compartments where each compartment can be tuned to match the characteristics of specific parts of the process.

Early results in controlling the clinker production are presented in Otomo, Nakagawa, and Akaike (1972), where statistical methods were applied to control the process. In Witsel, Barbieux, Renotte, and Remy (2005), simulation results of a multi-loop control scheme are presented. The model used to design the controller was previously presented in Spang III (1972), which is based on partial differential equations and includes heat transfer by convection and radiation, mass transport and reactions of water evaporation, calcination and clinker minerals formation. In Witsel et al. (2005) two PI controllers are designed to control a two input two output system. The PI controllers were parameterized based on a linear model identified by step responses from the model by Spang III (1972). It specifically excludes control of the oxygen level, which is important to guarantee combustion of the fuels. In Dumont and Belanger (1978a, 1978b), the successful control of a titanium dioxide kiln is presented. Even though the process relies on a rotary kiln too, the chemical reaction is significantly different (no exothermic component). Kim and Srivastava (1990), Koumboulis and Kouvakas (2003) and Mills, Lee, and McIntosh (1991) present simulation and application results for an industrial calciner, respectively. Again the chemical reaction is significantly different as calcination is purely an endothermic reaction. Additionally to temperature control the latter also controls CO–O_2 levels for combustion efficiency reasons.

All these works do not consider usage of alternative fuels. Today alternative fuels consisting of bone/carcass meal, whole tires, sewage sludge, house hold waste or solvents are of major importance to produce cement economically. The downside is that alternative fuels not only have a high variability in calorific value and combustion characteristics, they may also change the sintering process of the clinker. In Stadler, Wolf, and Gallestey (2007) a precalciner in the cement clinker production was controlled using a first principles model and model predictive control. This contribution explains how the models developed for that simpler application have been extended and adapted to address optimal control of a rotary kiln in the presence of alternative fuels.

Several aspects of this work are strongly influenced by the industrial setting. Typically, the lifetime of a cement plant is

* Corresponding author. Tel.: +41 58 586 81 79; fax: +41 58 586 73 65.
E-mail address: konrad.stadler@ch.abb.com (K.S. Stadler).

0967-0661/$ - see front matter © 2010 Elsevier Ltd. All rights reserved.
doi:10.1016/j.conengprac.2010.08.004

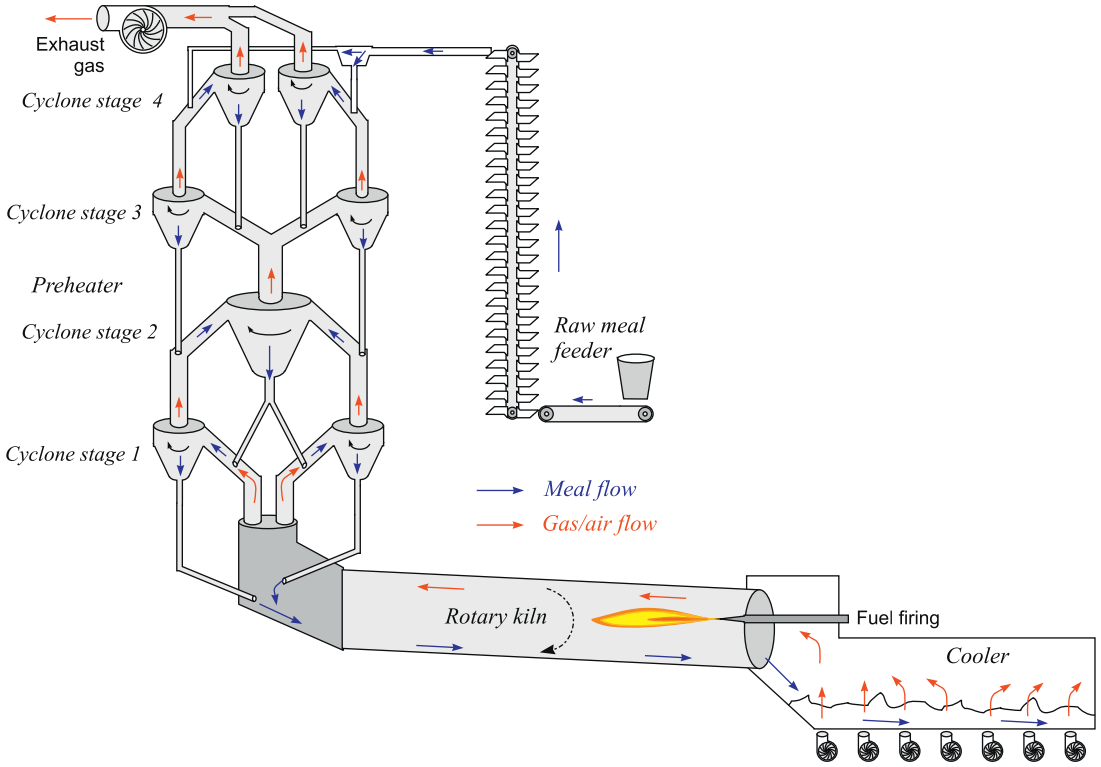

Fig. 1. Preheater kiln for the cement clinker production with four cyclone stages in the preheater tower, the rotary kiln and the cooler.

measured in decades and thus changes to the process structure are common. This means that also a kiln controller implementation needs to be easily adaptable to capture these changes. Moreover, for economic reasons it is a necessity that the controller can be easily adapted to serve different plants. The controller presented in this work was implemented on *cpmPlus Expert Optimizer* a commercial advanced process control and optimization platform developed by ABB.[1] The model is based on the mixed logic and dynamic (MLD) modeling approach (Bemporad & Morari, 1999) which is implemented in a graphical modeling environment. The graphical interface allows the model to be constructed from easily understandable and configurable submodels. Within the same modeling environment cost functions can be attached to formulate the optimization problem and to tune the controller performance all by dragging generic modeling elements from the library and dropping them on the model space (Stadler, Gallestey, Poland, & Cairns, 2009). The moving horizon estimation problem and the model predictive control problem are then generated automatically from this graphical representation.

The compartmental approach presented here meets these requirements because the whole estimation and control problem can be set-up by generic and predefined building blocks. Therefore, the complexity of the model and of the mathematical formulation can be hidden from the users. Additionally, the process depicts significant variability due to for example to diminishing of refractory lining of the kiln and changing chemistry of raw materials and fuels. The model needs to capture changes in the process dynamics sufficiently well to ensure that the controller operates over long periods without need of maintenance or re-tuning.

The paper is constructed as follows. In Section 3 the process and the basic equations of the model are presented. In Section 4 the formulation of the estimation and the control problem are given. Finally, in Section 5 results from the pilot site installation are described.

2. Process description

An overview of the cement production process can be found in Peray (1986) or Sahasrabudhe, Sistu, Sardar, and Gopinath (2006). In Fig. 1 the layout of a preheater kiln is shown. The preheater tower consists of several suspension cyclone stages where the feed and the exhaust gas from the combustion process further down the process exchange heat. The feed flows down the kiln and the gas is drawn upwards by a ventilator at the exhaust. The chemical composition of the raw feed needs to be controlled tightly to ensure good quality clinker; the main components are $CaCO_3$ (80%), SiO_2 (13%), AlO_3 (3%), Fe_2O_3 (2%) and MgO (1.6%). The feed temperature at the lowest cyclone stage reaches 800 °C or more. At this point calcination ($CaCO_3 + \text{heat} \rightarrow CaO + CO_2$) already has started (Peray, 1986).

Usually, at this stage in modern kilns a precalciner is introduced. Essentially, a precalciner is an additional combustion chamber, which is able to drive the dominant endothermic process of calcination. The more CO_2 from the raw material is released, the less work needs to be performed on the feed in the kiln, which increases the efficiency of the process greatly. The pilot plant presented in this work does not have a precalciner. This means that the calcination process needs to be driven by the heat in the exhaust gas from the main burner at the other end of the kiln. Decoupling of the dominant chemical reactions (calcination and sintering) is therefore not possible, which makes it intrinsically a more difficult process to control. The hot feed then enters the rotary kiln where its temperature is further increased. Between 1400 and 1500 °C, in the last third of the kiln, sintering of the clinker takes place. This is partially an exothermic reaction where the clinker compounds are formed (Peray, 1986). The clinker then drops onto the cooler which rapidly cools the clinker

[1] http://www.abb.com/cpm

down to approximately 150 °C by forcing ambient air through the clinker bed. This is important as cooling the clinker too slowly will allow the clinker minerals to revert to an un-sintered state. Moreover, significant heat is recuperated in the cooler for the process.

In Fig. 2 the temperature profile along the process is shown aligned with a qualitative description of the main chemical reactions taking place. The main control variables are the temperature profile along the process and the oxygen level (typically measured at the exhaust end of the preheater tower). These are chosen to directly influence the quality of the clinker and to ensure good combustion of the fuels, respectively. The manipulated variables are the air/gas draft through the kiln, the raw meal feed rate, the rotational speed of the kiln and the energy input by the fuels. Depending on the configuration of the plant at least one or more fuels can be manipulated (primary fuels). Typically, some alternative fuels are injected with the primary fuels at the same location. In the pilot site, in addition to the primary and alternative fuels firing at the front end of the kiln as indicated in Fig. 1, whole tires are dropped into the process at the kiln back end (i.e. where the meal feed enters the kiln); they burn while moving down the kiln with the feed.

The temperature profile as shown in Fig. 2 cannot be measured because along the rotary kiln temperature sensors are not available. Hence, estimating the temperature profile is an important issue and needs to be considered in the model design. Several unreliable or indirect indicators of the temperature in the burning zone are available. Typically three main indicators are used: the kiln torque, since the hotter the feed in the kiln gets, the more molten mass is being formed (Spang III, 1972). Therefore the feed is dragged up further by the rotation and hence the required torque to rotate the kiln at constant speed will increase; a pyrometer signal (very unreliable because of the dusty environment) at the kiln outlet; and NO_x readings (higher gas temperatures increase the probability of NO_x formation during the combustion) in the exhaust gas (Peray, 1986). Typically, for reliability at least two of these measurements are aggregated by a soft sensor to form a single burning zone indicator (Lobier, Taylor, & Kemmerer, 1989) named burning zone temperature (BZT). Furthermore, gas temperature readings from various cyclone stages are available.

3. Model of a rotary cement kiln

To derive the temperature profile of the feed and the gas it is necessary to describe the thermodynamic relations along the process. The thermodynamic behavior is driven by the corresponding chemical reaction within the parts of the process, preheating, calcining, sintering, and cooling, hereafter referred to as *zones*. To simplify the overall thermodynamic modeling of the process, the system is divided into compartments corresponding to the zones in Fig. 2. Dividing the process into segments has been described previously, see Kääntee, Zevenhoven, Backman, and Hupa (2002) and Locher (2002). The resulting models were only used to simulate the process, and therefore the process was divided into many segments to increase the accuracy of the model fit. In this paper the goal is to use a sufficiently accurate model for closed loop control which typically does not require (or permit, for observability and computational reasons) the same level of detail and accuracy as simulation models. Here a model structure similar to Fleeman, Kaiser, Lane, and Mahoney (1966) is used. Essentially, the process is segmented into the same five zones or compartments: the four mentioned so far and a transition zone inserted between calcining and sintering. In contrast to Fleeman et al. (1966), each compartment is further divided into meal and gas phase states, without wall states.

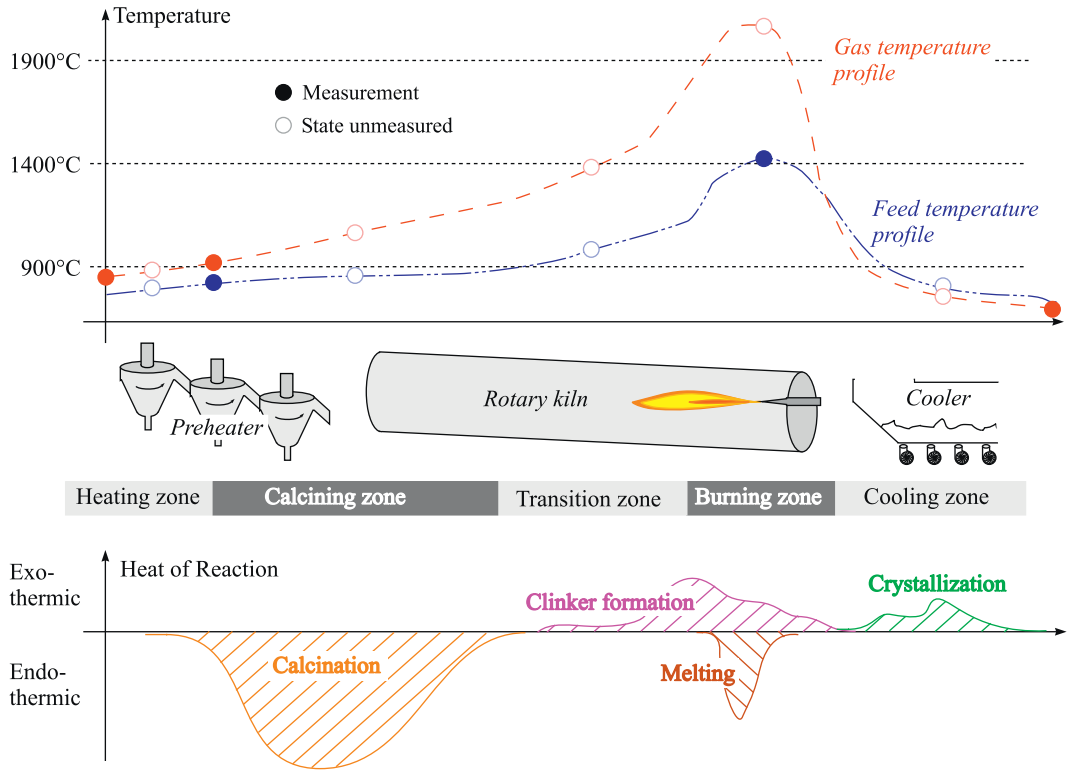

Fig. 2. Temperature profile and the qualitative profile of the heat of reaction of the feed along the clinker production unit.

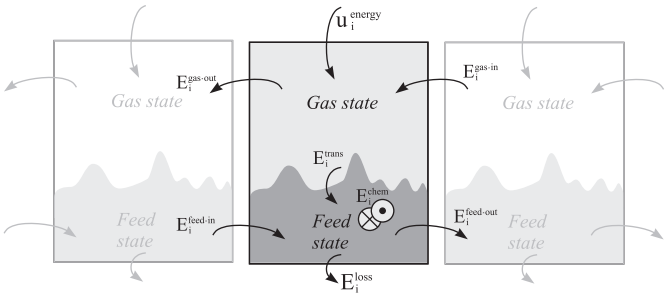

Fig. 3. The kiln is modeled by interconnecting thermal compartments. The feed and gas temperature states are denoted by feed and gas state, respectively.

The behavior of the compartments (Fig. 3) is described by an energy and mass balance. It has energy sources and energy sinks related to

- feed and gas transport,
- combustion of fuels (where appropriate),
- losses to the ambient,
- energy sources or sinks related to the chemical reactions.

The thermodynamical processes considered here are non-linear. However, for estimation and control, a linearized version of the model will be used. Some of the changes needed to obtain a linear model make the equations simpler, while others make the equations more complex. The former are incorporate immediately in the model below while the latter are postponed.

For each compartment $i \in \{1,\ldots,K\}$ the corresponding equations are:

Mass transport dynamics.

$$\dot{\overline{\mathbf{m}}}_i^f = \frac{1}{L_i}(\mathbf{u}_i^{fin} - \overline{\mathbf{m}}_i^f \cdot \mathbf{u}_i^V) \tag{1}$$

The mass state $\overline{\mathbf{m}}_i^f$ (not shown in Fig. 3) describes the actual feed mass density within the compartment. Homogenous mass distribution is assumed within the compartment. This approximation reduces the complexity of the model significantly. The equation is important for the transport dynamics of the feed and therefore is part of the heat transport dynamics. The dynamic behavior depends on the length L_i of the compartment, the feed input rate $\mathbf{u}_i^{fin}$ and the feed output rate. The feed output rate depends on the mass state $\overline{\mathbf{m}}_i^f$ and the feed transport velocity $\mathbf{u}_i^V$. The latter is proportional to the kiln rotary speed.

Feed temperature dynamics.

$$c^f \overline{\mathbf{m}}_i^f \dot{\mathbf{T}}_i^f = \overbrace{\frac{c^f \mathbf{u}_i^{fin}}{L_i}(\mathbf{u}_i^{T_{fin}} - \mathbf{T}_i^f)}^{\mathrm{E}_i^{\text{feed-in}} - \mathrm{E}_i^{\text{feed-out}}} + \overbrace{k_i^t(\mathbf{T}_i^g - \mathbf{T}_i^f)}^{\mathrm{E}_i^{\text{trans}}} + \overbrace{\frac{\mathbf{u}_i^V \overline{\mathbf{m}}_i^f k_i^c}{L_i}}^{\mathrm{E}_i^{\text{chem}}} - \overbrace{\frac{k_i^l \mathbf{T}_i^f}{L_i}}^{\mathrm{E}_i^{\text{loss}}} \tag{2}$$

The feed temperature state $\mathbf{T}_i^f$ describes the heat stored in the feed within the corresponding compartment. According to the heat flows shown in Fig. 3 the dynamic equation is formulated. The main assumptions are that the chemical reaction of the clinker process is constant within a compartment and that the heat loss of the whole system is proportional to the feed temperature state only. Moreover, the feed heat distribution within the compartment is assumed homogeneous and the modeled heat transfer between gas and feed temperature state is governed by a linear relation, see below.

Gas temperature dynamics.

$$c^g \overline{m}^g \dot{\mathbf{T}}_i^g = \overbrace{\frac{c^g \mathbf{u}^{g_{flow}}}{L_i}(\mathbf{u}_i^{T_{gin}} - \mathbf{T}_i^g)}^{\mathrm{E}_i^{\text{gas-in}} - \mathrm{E}_i^{\text{gas-out}}} - \overbrace{k_i^t(\mathbf{T}_i^g - \mathbf{T}_i^f)}^{\mathrm{E}_i^{\text{trans}}} + \overbrace{\frac{1}{L_i}\mathbf{u}_i^{fuel}}^{\mathrm{u}_i^{\text{energy}}} \tag{3}$$

The gas temperature state $\mathbf{T}_i^g$ describes the heat stored in the gas within the corresponding compartment. According to the heat flows shown in Fig. 3 the dynamic equation is formulated. The main assumption is that the energy input of the fuels occurs into the gas state only. Again, the gas heat distribution within the compartment is assumed homogeneous and the modeled heat transfer between gas and feed temperature state is governed by a linear relation, see below.

The compartment states are:

$\overline{\mathbf{m}}_i^f$	(t/m)	average mass density
$\mathbf{T}_i^f$	(°C)	feed temperature
$\mathbf{T}_i^g$	(°C)	gas temperature

The compartment inputs are:

$\mathbf{u}_i^V$	(m/h)	feed transport velocity (typically $\propto$ kiln rotary speed)
$\mathbf{u}_i^{fuel}$	(MJ/h)	energy released by burning fuels
$\mathbf{u}_i^{g_{flow}}$	(t/h)	gas flow (typically related to exhaust fan speed)
$\mathbf{u}_i^{fin}$	(t/h)	feed input
$\mathbf{u}_i^{T_{fin}}$	(°C)	input feed temperature
$\mathbf{u}_i^{T_{gin}}$	(°C)	input gas temperature

The compartment parameters are:

L_i	(m)	compartment length
c^f	(MJ/t°C)	specific heat capacity of meal feed
c^g	(MJ/t°C)	specific heat capacity of gas or air
$\overline{m}^g$	(t/m)	average mass density of gas or air state
k_i^l	(MJ/h)	energy loss in the compartment
k_i^c	(MJ/t)	energy source (+) or sink (−) due to chemical reaction
k_i^t	(MJ/mh°C)	heat transfer coefficient between gas and feed state

Experienced process engineers can typically separate the zones along the kiln and therefore the length of the compartment can be approximated.

Heat transfer in rotary kilns are typically related to radiation and a mixture of convection and conduction (Boateng, 2008). Radiation is governed by the Stefan–Boltzmann law, i.e. between the gas and the feed state the heat transfer is proportional to $[(\mathbf{T}_i^g)^4 - (\mathbf{T}_i^f)^4]$. Conduction and convection occur typically in conjunction (Boateng, 2008) and can be modeled by the concept of thermal resistance, i.e. heat transfer is therefore proportional to $[\mathbf{T}_i^g - \mathbf{T}_i^f]$. For control purposes, a linearized model will be used, resulting in a linear description for the heat transfer

$$\mathrm{E}_i^{\text{trans}} = k_i^t[\mathbf{T}_i^g - \mathbf{T}_i^f]$$

This greatly simplifies the linearization of the model.

Average specific heat capacities for gas and feed are known from the literature (Spang III, 1972). The average mass density $\overline{m}^g$ of the gas air state is a tuning parameter and relates to the dynamics of the gas state time constant. In comparison to the feed dynamics the gas dynamics are considerably faster. For control purposes the gas dynamics are not critical as the overall clinker

quality is related to the mass state. To simplify the system, the gas mass in the compartment is set constant. Typical temperature profiles at steady state for many different types of rotary kilns are known (Peray, 1986). The parameters k_i^l, k_i^c and k_i^t are tuning parameters and can be used to reproduce the desired temperature profile. Nevertheless, the approximate range for k_i^l and k_i^c can be found in the literature (Alsop & Post, 1995; Boateng, 2008).

Oxygen dynamics. In addition, the overall model includes a simple oxygen model to describe the oxygen content in the exhaust gas ($\mathbf{O}$) to ensure combustion conditions

$$\dot{\mathbf{O}} = a^{oxy}\mathbf{O} + k^{oxy}\mathbf{u}^{g_{flow}} - c^{oxy}\mathbf{u}^{fuel} \tag{4}$$

The sensor dynamics are described by the parameter a^{oxy}. Moreover, the parameters k^{oxy} and c^{oxy} relate the oxygen source by the gas/air draft through the system and the oxygen sink by the combustion, respectively.

4. Control problem formulation

4.1. Model linearization

The model described above is nonlinear and within the current framework of the controller platform only piecewise linear systems can be addressed. In this type of process the operating point is not changed for longer periods (the objective with highest importance is to maximize throughput). Therefore, it is reasonable to linearize the nonlinear expressions of the first principles model. Thus the linearization points become a set of parameters containing parts that correspond to states and parts that correspond to the inputs. They are accordingly denoted by $\binom{x^0}{u^0}$. For the observability argument below it is important to know that the mass states in the denominator of the temperature evolution are not linearized but *replaced* by the current linearization point. The bilinear expressions $\mathbf{x}_i\mathbf{x}_j$ are approximated by $\mathbf{x}_i x_j^0 + x_i^0\mathbf{x}_j - x_i^0 x_j^0$.

4.2. Moving horizon state estimation

The model has one oxygen state (Eq. (4), $\mathbf{O}$) and three states for each of the five compartments. These are the mass density (Eq. (1), $\overline{\mathbf{m}}_i^f$) the feed temperature (Eq. (2), $\mathbf{T}_i^f$) and the gas temperature (Eq. (3), $\mathbf{T}_i^g$). However, at worst there are only three measurements available (temperature at the back end (BET), temperature in the burning zone (BZT), and oxygen after combustion (O2)). In Fig. 2, the unmeasured and the measured states are marked with empty and filled circles, respectively. Thus, state estimation is clearly required to derive the current states and to apply standard receding horizon control. *Moving horizon estimation* (MHE) was used for this purpose (Rao, 2000). In MHE, an optimization problem involving the model over a certain horizon is established and solved, similar to the receding horizon control problem. Here, the horizon extends N steps into the past, and the objective of the optimization is to determine the states such that the measurements and the state evolution are met, i.e. making a trade off between confidence in the observations and confidence in the model equations. A MHE problem based on a linear model including constraints can be formulated as follows:

$$\begin{aligned} \min_x \quad & \sum_{k=-N}^{-1} \{\|y^{obs}[k] - (Cx[k] + Du[k])\|_R^2 + \|x[k+1] - (Ax[k] + Bu[k])\|_Q^2\} \\ \text{s.t.} \quad & Sx[k+1] = S(Ax[k] + Bu[k]) \\ & -E_5 \le E_4 x[k] + E_1 u[k] \end{aligned} \tag{5}$$

Here, the model is given in standard form by the matrices A, B, C, D and the state vector $x[k]$ consists of the states $\overline{\mathbf{m}}_i^f$, $\mathbf{T}_i^f$, $\mathbf{T}_i^g$ and $\mathbf{O}$. Moreover E_1, E_4, E_5 define the constraints (this notation is a subset of the MLD formulation in Bemporad & Morari, 1999). In this case the constraints are state and input constraints. The matrices R and Q used in the norms are the weight matrices for measurement error and dynamic equation error, respectively. The matrix S is used to enforce exact state evolution for certain states. It contains as many rows as there are states to evolve according to the dynamic equation; each row contains a one for a state evolved without state noise and zeros for all other states.

4.3. Capturing model uncertainty

In addition to state estimation, the optimization problem equation (5) can be used to detect systematic deviations of the plant observations from the modeled dynamics, and thus compensate for disturbances. If for instance the raw meal entering the kiln requires more energy for calcining than expressed by the model parameter, then the temperature measurements will be consistently lower than expected by the model. The model was augmented with an additional state that implements additive correction to the energy required for calcination. This *adaptive correction term* can be estimated as part of the optimization problem in Eq. (5). As long as no other evidence suggests differently, the undisturbed evolution of this adaptive term is $x_{t+1} = x_t$ and it will respond to any disturbance which can be related to temperature deviations.

For all available measurements (BET, BZT, O2), an additive term was placed on states close to the corresponding measurement resulting in additive corrections of the corresponding state evolution. Using more adaptive terms than measurements available is risky without imposing additional structure, since then there might be no unique estimation result, and the estimator might start oscillating. Using fewer adaptive terms than measurements can be sensible if it is not desired to exploit the opportunity to identify model mismatch.

4.4. Reducing the estimation problem

Given the observations (BET, BZT, O2) and the linearized model equations, and recalling the remark on the mass state at the end of Section 4.1, it is clear that the mass state is not observable. However, the mass transport model is (assumed to be) sufficiently accurate such that open-loop simulation is reasonably accurate. Hence the mass states are open-loop simulated and used in the state estimation equations in the following way whenever they occur: A vector of historical values is stored for each mass state, and these values are inserted at the appropriate places in the equations. All evolution equations corresponding to these *simulated states* will be equipped with a very small weight (large state noise) and thus factually disabled.

The linearized kiln model with removed mass states has been found observable according to the standard criteria. However, in practice, model mismatch can lead to poor performance and oscillations of the estimator. In order to make the estimator more robust, the estimation problem was further reduced: In addition to the mass states, also temperature states in the transition zone and in the cooling zone are *simulated* externally. In this way the temperature estimation problem is split into two independent subproblems, one at the back end and one in the burning zone of the kiln (Poland, Isaksson, & Aronsson, 2009, Section 2.4).

4.5. Optimal control problem

The optimal control problem is formulated in a standard way, where the notation is again a subset of the MLD formulation in Bemporad and Morari (1999):

$$\begin{aligned}\min_{x,u,z} \quad & \sum_{k=0}^{M-1} \{\|y^{ref}[k]-(Cx[k]+Du[k])\|_W^2, \ldots \\ & +L(Cx[k]+Du[k])+\|z\|_{W_z}^2+L_z z[k]\} \\ \text{s.t.} \quad & x[k+1]=Ax[k]+Bu[k] \\ & x[0]=x^{start} \\ & E_3 z[k] \le E_4 x[k]+E_1 u[k]+E_5 \end{aligned} \tag{6}$$

The parameter M describes the receding control horizon. Here, $z[k]$ is a vector of auxiliary variables at each time step used to define soft constraints and 1-norms. Note that the design of the cost function should be according to the targets of the respective plant. Using auxiliary variables, it is easy to penalize for instance low oxygen levels only if the oxygen state **O** drops below a certain limit o^{low}, but then penalize it strongly. This is implemented by introducing an auxiliary variable z_1 and a constraint of the form $\mathbf{O} \ge o^{low}-z_1$ and adding a linear and/or a quadratic function of z_1 to the cost expression. Hence, by introducing auxiliary variables asymmetric cost functions or cost functions with dead band can be easily realized.

The matrices W, L, W_z and L_z define the quadratic and linear costs of states and auxiliary variables, respectively. Because the manipulated variables are formulated as incremental differences and integrated within the model, the rate constraints can be formulated as input constraints. In fact, the above formulation does not cover all of what is expressible in the used control platform *cpmPlus Expert Optimizer*, but it is sufficient to express what has been used for the experiments described below. Note all states related to adaptive terms attain and preserve the respective values returned by the estimation.

Fig. 4 shows the kiln model and associated controller as they appear inside the cpmPlus Expert Optimizer platform. Note the compartmental structure, which is adapted graphically according to the structure of the real plant.

5. Results

The controller was commissioned on a cement plant in Switzerland (Holcim Ltd., Plant Siggenthal). Since finalizing the commissioning in mid-2007 the controller has an average uptime of more than 95%.

Fig. 5 shows a period of 10 days where the controller was active. During this period the uptime of the controller was 97.9%. The main process variables (BZT, O2 and BET) with their corresponding references are shown along with the main manipulated variables (feed rate and specific energy input). The cost function specifications are implemented as soft constraints and additionally the BET and the O2 are given a reference range indicated by low and high values describing the soft constraint. The high limit of the oxygen constraint is outside the range shown on this plot. The controller nicely keeps the process variables within the desired ranges while keeping the feed rate close to the maximal feed rate.

Validation of controllers in an industrial setting is difficult as the variability of the influences from outside are significant. For example the plant considered here uses up to 40% alternative fuels which are delivered daily to the plant. The variability of the fuel (calorific value, water content) and the fuel mix will change several times a day depending on the availability of the alternative fuels. The influence on the process is difficult to assess. The combustion characteristic of each fuel will affect the combustion characteristic of the fuel mix which will greatly influence the sintering conditions in the kiln.

Nevertheless, it is important to get a feeling on the potential benefit a control system like the one presented here may have in comparison to manual operation.

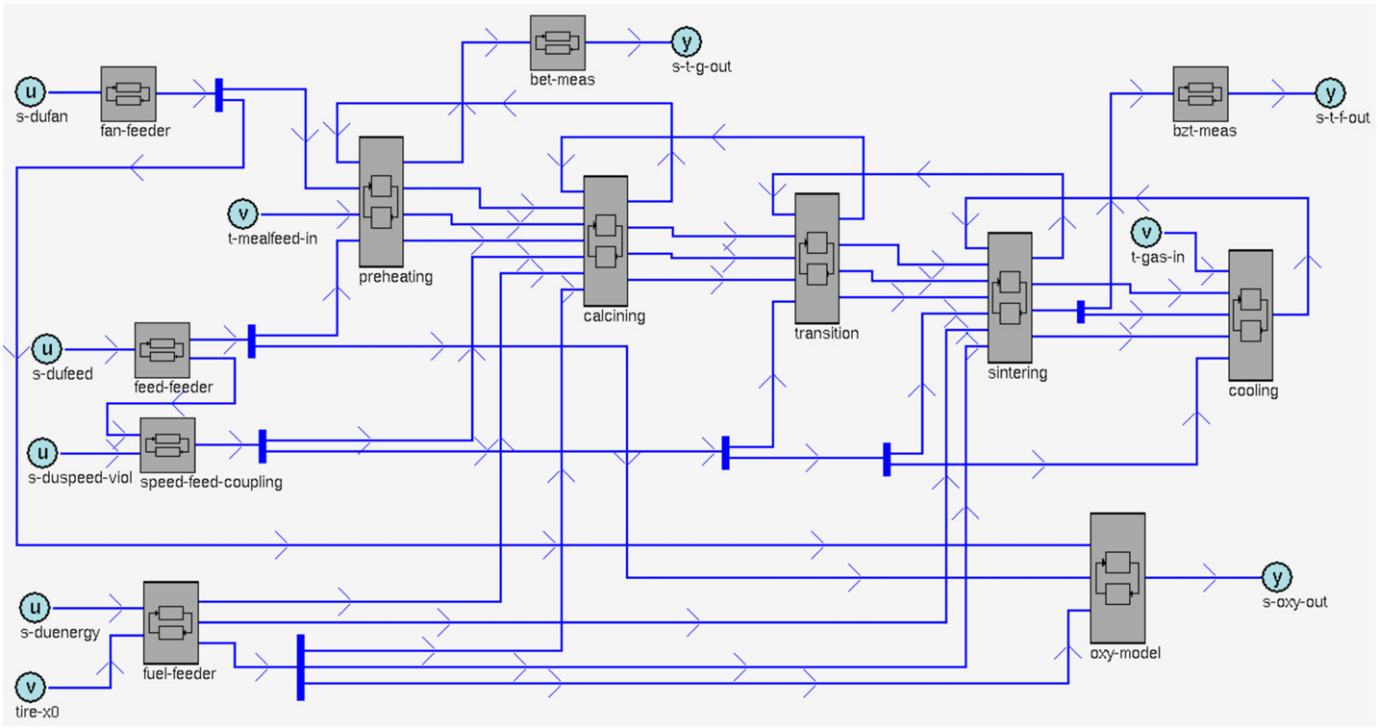

Fig. 4. Kiln model and controller inside the cpmPlus Expert Optimizer platform.

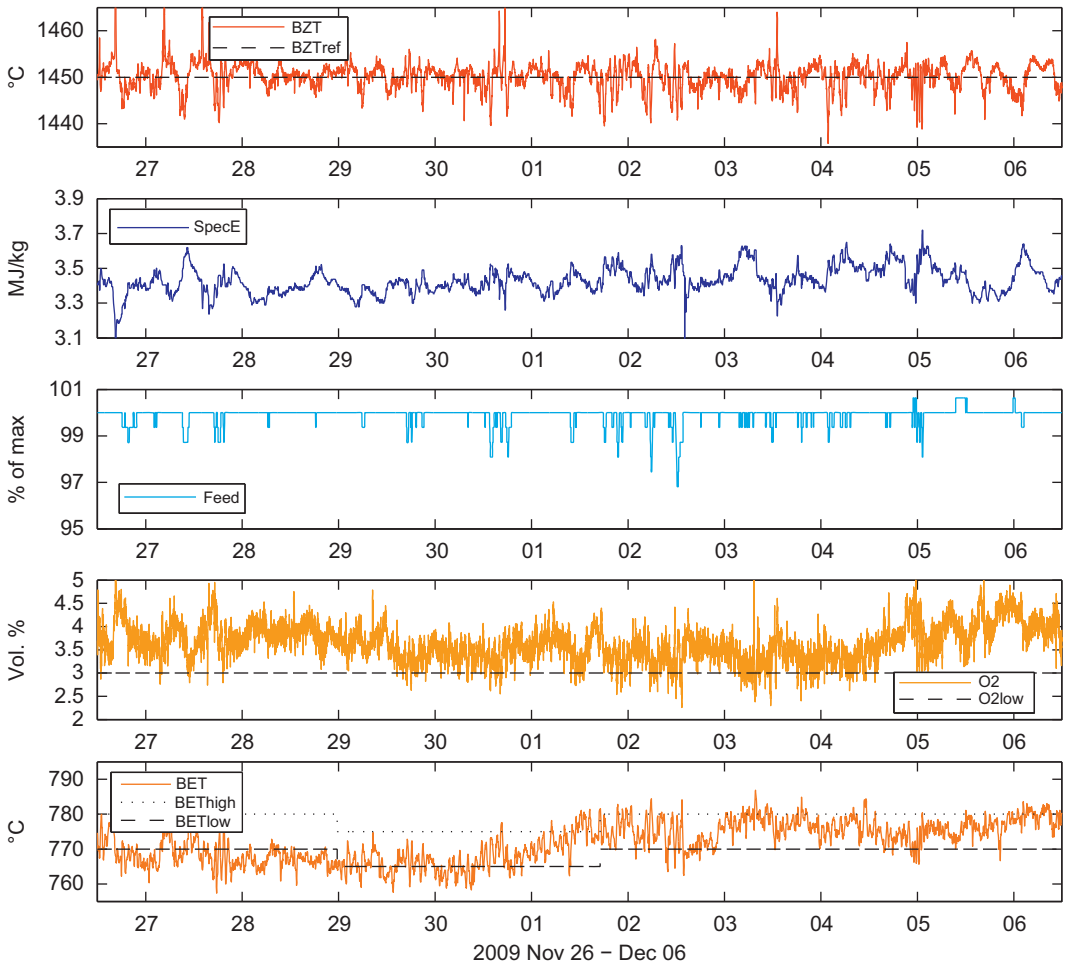

Fig. 5. Top subplot: burning zone temperature (BZT, solid) and reference (BZTref, black, dashed); second subplot: feed rate in percentage of maximal feed rate; third subplot: specific energy input (SpecE); fourth subplot: oxygen level in the preheater tower (O2, solid) and lower soft constraint value (O2low, dashed); lower subplot: back end temperature (BET, solid) and lower (BETlow, dashed) and higher (BEThigh, dotted) constraint value.

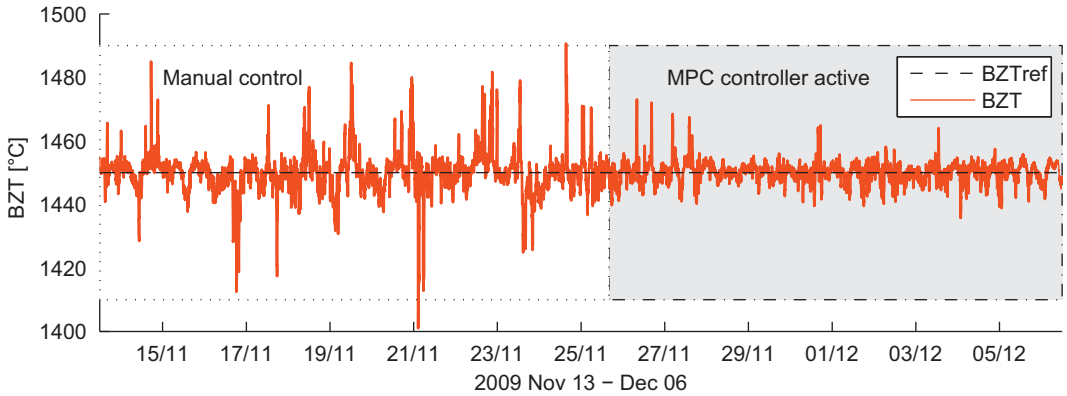

Fig. 6. Burning zone temperature (BZT, solid) and its reference (BZTref, dashed). The grey background indicates where the MPC controller was active.

In Fig. 6 the burning zone temperature is shown for a period between November 13th and December 6th 2009. In the first half of the period the controller was not used and in the second half of the period the controller was used. The reduction in variability of the burning zone temperature is apparent.

For validation a 10 days period where the controller was offline (i.e. the operators controlled the kiln manually) and a 10 days period where the controller was online was selected and several key performance indicators where evaluated. The offline and the online periods are named MANCtrl and MPCCtrl, respectively. During the online periods the controller occasionally has to be taken offline for a few minutes when for example a required measurement is not available or when the operators have to switch to manual while maintenance on an actuator or sensor is carried out. Still, the accumulated offline time during the 10 days MPCCtrl period considered amounts to just over 5 h. However, for the evaluation of the key performance indicators these short "offline" gaps are considered as part of the "online"

period because the effect on the indicators is negligible. The key performance indicators are summarized in Table 1.

Statistically, there is no significant difference between the mean values of the key performance indicators. The MPC controller shows an improved performance for the feed rate and on average lower oxygen levels. The latter is surprising as the specific energy used in the MPCCtrl period is slightly higher than for the MANCtrl period. Generally, it is expected that lower oxygen levels would indicate that the kiln was less over-drafted and therefore less energy would be lost with the exhaust gas. Moreover, the lower BET also is an indicator that the losses through the exhaust gas should be lower. Hence, all this should result in a lower specific energy consumption. On the contrary, the specific energy consumption is calculated by using highly uncertain information on the calorific values of the alternative fuels. These are typically monthly averages of samples taken when the fuels are delivered and large deviations are known.

Table 1
Key performance indicators (KPI) for MANCtrl and MPCCtrol periods.

Period	KPI (Unit)	Mean	SD	LL	HL
MPCCtrl	Feed rate (%)	99.8	0.36		
MANCtrl	Feed rate (%)	97.6	11.88		
MPCCtrl	O2 (Vol%)	3.65	0.39	3.9%	
MANCtrl	O2 (Vol%)	3.80	0.93	2.8%	
MPCCtrl	SpecE (kJ/kg)	3428.8	76.1		
MANCtrl	SpecE (kJ/kg)	3414.4	439.9		
MPCCtrl	BET (°C)	771.9	5.6	29.6%	8.6%
MANCtrl	BET (°C)	773.4	8.6	26.9%	8.8%
				$\mathbf{R} \pm 1/2\%$	$\mathbf{R} \pm 1\%$
MPCCtrl	BZT (°C)	1450.2	2.94	97.7%	99.8%
MANCtrl	BZT (°C)	1450.0	6.38	86.7%	95.6%

The Feed rate is the percentage of maximal possible feed rate, O2 is the oxygen level in the preheater tower, SpecE is the specific energy used (energy per kg of produced clinker), BET is the back end temperature and BZT is the burning zone temperature. For all KPIs the mean and the standard deviation (SD) and where appropriate, the percentage of measurements below the low limit (LL), the percentage of measurement above the high limit (HL), the percentage of measurements within $\pm 1/2\%$ ($R \pm 1/2\%$) or $\pm 1\%$ ($R \pm 1\%$) of the reference is given.

Considerable improvements are observed when examining the standard deviations. All standard deviations are considerably reduced, which confirms the result shown in Fig. 6. The percentage of measurements outside the low and high limits is of similar size. The percentage of measurements within the defined ranges $R \pm 1/2\%$ and $R \pm 1\%$ of the reference value for the burning zone temperature is considerably higher.

In Fig. 7 the histograms of the main process variables are shown. The control error (ΔBZT) shows a narrower distribution for MPCCtrl than for MANCtrl. Both the MANCtrl and the MPCCtrl distribution are skewed with a longer tail towards negative deviations, i.e. to lower absolute temperatures. Because the skewness also appears in the MANCtrl distribution it may originate in the nonlinear function to derive the burning zone temperature. As the BET is a true temperature measurement it shows close to normal distribution for the MANCtrl period. However, the MPCCtrl period shows a distribution with two peaks, one located at the lower BET constraint value and one at the higher BET constraint value, respectively. This is a classical result of the optimization as it typically pushes a process variable which is bounded with a soft constraint to either of the limits.

The oxygen in the preheater is distributed nearly identically for the MANCtrl and MPCCtrl periods. The distribution of the main control variable, the energy input (given here as the specific

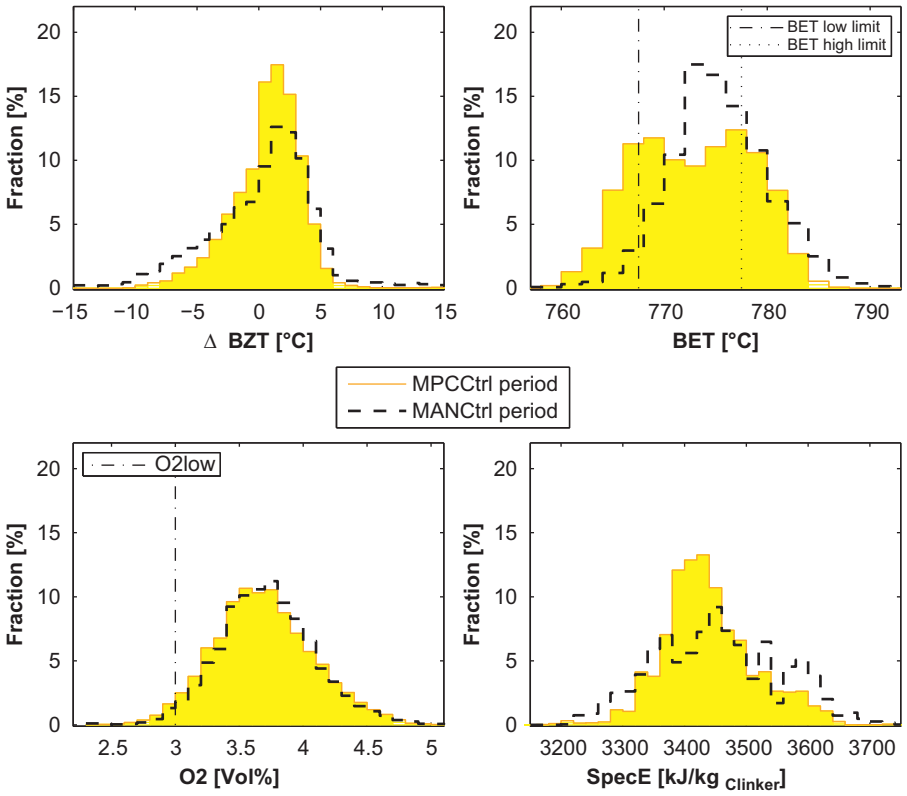

Fig. 7. Histograms of the difference between target temperature and burning zone temperature (ΔBZT), the back end temperature (BET), the oxygen level in the preheater (O2) and the specific energy (SpecE). On the ordinate the fraction of measurements within the corresponding bins are given.

energy) is considerably narrower for the MPCCtrl than the MANCtrl period. Moreover, the distribution of the MANCtrl period does not show a nice smooth distribution. This could indicate that the operators tend to "overreact" resulting in less stable process conditions.

6. Conclusion

The first principles model presented here is implemented in linearized form on a commercial advanced process control platform. Model parameter changes are captured by aggregating all the uncertainty into few variables only, which is sufficiently robust as shown by the results. Parameter and state estimation is carried out in a combined estimation, which is formulated as a moving horizon estimation problem.

The controller was commissioned on a cement plant and it has been in operation close to two years with highly satisfactory performance. The controller performance evaluation is in accordance with the tuning of the corresponding cost functions.

The controller comparison to manual control needs to be assessed with care. However, general trends can be readily seen. The variability of the process and manipulated variables have been considerably reduced by using the MPC controller presented here. This as such – without considering higher production rates – is a benefit for the plant in many ways. For example more stable process conditions mean lower risk of blockages in the preheater cyclones. Blockages within the cyclone mean production shutdowns, maintenance activity and poor clinker quality during restart phases. Moreover, more stable process conditions mean also lower thermal stress on the equipment and therefore less ware especially for the refectory lining of the rotary kiln. The difference between manual control by the operator and the MPC controller described here is that the latter controls the process with regular and typically much shorter intervals and therefore also with smaller control moves. This is reflected in the more stable process conditions while simultaneously the throughput is maximized.

Acknowledgements

The authors wish to thank the management and staff of Holcim Ltd., Plant Siggenthal for the fruitful discussions and continuous support during commissioning of the controller.

References

Alsop, P. A., & Post, J. W. (1995). *Cement plant operations handbook* (1st ed.). Tradeship Publications Ltd.

Bemporad, A., & Morari, M. (1999). Control systems integrating logic, dynamics and constraints. *Automatica*, *35*(3), 407–427.

Boateng, A. A. (2008). *Rotary kilns transport phenomena and transport processes*. Butterworth-Heinemann.

Dumont, G. A., & Bélanger, P. R. (1978a). Control of titanium dioxide kilns. *IEEE Transactions on Automatic Control*, *AC-23*(4), 521–531.

Dumont, G. A., & Bélanger, P. R. (1978b). Self-tuning control of a titanium dioxide kiln. *IEEE Transactions on Automatic Control*, *AC-23*(4), 532–538.

Fleeman, P. J., Kaiser, V. A., Lane, J. W., & Mahoney, J. D. (1966). Process control systems for reactors. GB Patent No. 1,052,333, priority date May 2, 1963 based on US Patent Application 277,625, December.

Kääntee, U., Zevenhoven, R., Backman, R., & Hupa, M. (2002). Modelling a cement manufacturing process to study possible impacts of alternative fuels. In: *TMS fall 2002 extraction and processing division meeting on recycling and waste treatment in mineral and metal processing: technical and economic aspects*, Lulea, Sweden, June.

Kim, N. K., & Srivastava, R. (1990). Simulation and control of an industrial calciner. *Industrial & Engineering Chemistry Research*, *29*(1), 71–81.

Koumboulis, F. N., & Kouvakas, N. D. (2003). Model predictive temperature control towards improving cement precalcination. *Proceedings of the Institution of Mechanical Engineers, Part I: Journal of Systems and Control Engineering*, *217*(2), 147–153.

Lobier, G., Taylor, R., & Kemmerer, J. (1989). Supervisory control applied to a cement kiln incinerating recovered solvent. In *IEEE cement industry technical conference* (pp. 275–283), 1989, XXXI, Denver, CO, May.

Locher, G. (2002). Mathematische Modelle zum Prozess des Brennens von Zementklinker. Teil 3: Drehrohrofen. *ZKB International (Cement-Lime-Gypsum)*, *55*(3), 68–80.

Mills, P. M., Lee, P. L., & McIntosh, P. (1991). A practical study of adaptive control of an alumina calciner. *Automatica*, *27*(3), 441–448.

Otomo, T., Nakagawa, T., & Akaike, H. (1972). Statistical approach to computer control of cement rotary kilns. *Automatica*, *8*(1), 35–48.

Peray, K. E. (1986). *The rotary cement kiln* (2nd ed.). New York, NY: Chemical Publishing Co., Inc.

Poland, J., Isaksson, A. J., & Aronsson, P. (2009). Building and solving nonlinear optimal control and estimation problems. In *Proceedings 7th Modelica conference* (pp. 39–46), Como, Italy, September.

Rao, C. V. (2000). *Moving horizon strategies for the constrained monitoring and control of nonlinear discrete-time systems*. Ph.D. thesis, University of Wisconsin.

Sahasrabudhe, R., Sistu, P., Sardar, G., & Gopinath, R. (2006). Control and optimization in cement plants. *IEEE Control Systems Magazine*, *6*(26), 56–63.

Spang, H. A., III (1972). A dynamic model of a cement kiln. *Automatica*, *8*(3), 309–323.

Stadler, K. S., Gallestey, E., Poland, J., & Cairns, G. (2009). Optimal trade-offs—achieving energy efficiency and environmental compliance is not a problem thanks to advanced process control. *ABB Review 2|2009*, 17–22.

Stadler, K. S., Wolf, B., & Gallestey, E. (2007). Precalciner control in the cement production using MPC. In *Proceedings of the 12th IFAC symposium on automation in mining, mineral and metal processing. International federation of automatic control* (pp. 201–206), Québec City, Canada, August 21–23.

Witsel, A.-C., Barbieux, V., Renotte, C., & Remy, M. (2005). Multi-loop control scheme of a cement kiln. In *Proceedings of the 24th IASTED international conference modelling, identification and control* (pp. 217–222), Innsbruck, Austria, February.